

# A Novel Microrheometer for Measuring Rheological Properties of Microquantities of Fluids

C.S. Lo<sup>1</sup>, P. D. Prewett, M.C.L Ward and P. T. Docker

University of Birmingham, Research Centre for Micro-Engineering and Nanotechnology, Birmingham,  
B15 2TT, UK  
<sup>1</sup> [csl821@bham.ac.uk](mailto:csl821@bham.ac.uk)

## ABSTRACT

A novel micromachined microrheometer is designed to measure the rheological properties of microquantities of fluid. The measuring principle of this device is based on the interaction of electromagnetic field, superparamagnetic microbeads and fluids. A simple model is developed to test the behaviour of the superparamagnetic microbead with various fluid viscosities.

**Keywords:** Microrheometer, electromagnetic field, superparamagnetic microbead.

## 1 INTRODUCTION

The main motivation in microrheology studies is to understand the rheological behaviour of elastic liquids such as the polymer melts and polymer solutions associated with the synthetic fibre and plastic industries. The dramatic decrease in sample volume makes it feasible to perform rheological measurements in situations where only a limited amount of material is available. [1]

Current techniques include oscillatory thermorheometry (OTR) used to correlate microquantities of fluid by applying constant oscillatory forces with yield steady-shear viscosity and viscoelastic moduli [2, 3]. Another method uses AFM in which the cantilever tip is used to indent the surface of a sample and sinusoidal modulations are superimposed to measure frequency dependent mechanical responses that can be interpreted in terms of elastic and viscous dynamic moduli. [4, 5]

This paper first explains the measuring principle of the device, how it will be made before giving preliminary results and finally the paper's conclusions.

## 2 MEASURING PRINCIPLE

The microrheometer consists of an array of electromagnetic microcoils and a microfluidic channel. The microcoils generate a magnetic force to control the movement of the superparamagnetic beads. The microfluidic channel provides a reservoir, which channels the flow of the beads within the fluid. The device is coupled with a pair of external magnets which polarize and saturate the magnetic beads.

Initially the channel will be filled with a known

fluid content mixed with a measured volume of superparamagnetic beads. The microbeads are polarized by exposure to the magnetic field,  $\vec{B}_{ext}$  generated from an external permanent magnet (NdFeB). The dipole moment appears when the bead is polarized. A DC current is passed through the microcoils, which creates a magnetic field gradient and thus a magnetic force on the beads. The movements of the microbeads are controlled when the current is switched alternately through each individual microcoil. The viscosities of different fluids are measured through the time of flight of the microbead traveling over a distance of 100 μm.

In most practical cases it is necessary to determine the magnetization and the susceptibility of a substance in a homogeneous magnetic field,  $\vec{B}_{ext}$  [6]:

$$\vec{m} = \frac{\chi_v V \vec{B}_{ext}}{\mu} \quad (1)$$

where  $\vec{m}$  is the magnetization,  $\chi_v$  is the volume susceptibility,  $\mu$  is the permeability of free space and  $V$  is the volume of the bead. In this model we assume the use of hydrophobic M-450 superparamagnetic microbeads from Dynal has been used. These are made from ferric oxide ( $Fe_2O_3$ ) powdered iron core in polymer matrix. The radius of the microbead,  $R_{bead}$  is 2.25 μm with a bulk magnetic susceptibility of  $10 \times 10^{-4} m^3/kg$ . The volume susceptibility of the magnetic bead can be written as [7]

$$\chi_v = \chi_p \cdot \rho \quad (2)$$

where  $\rho$  is the density of a single bead and  $\chi_p$  is the bulk magnetic susceptibility. The total magnetic flux density,  $\vec{B}_{coil}$  for a coil can be obtained from the Biot-Savart Law in the form of [8]:

$$\vec{B}_{coil} = \frac{\mu_0}{4\pi} \int \frac{Idl \times \vec{a}_R}{a^2} \quad (3)$$

The unit vector specifies the vector  $\vec{a}_R$  from the source to the field point.  $Idl$  represents the differential current element in the same direction as the current in the coil and  $a$  is the distance from the source to the field point. In order to observe the magnetic field produced from a coil,  $\vec{B}_{coil}$  can

be written in the magnetic vector potential form as [8]:

$$\vec{B}_{\text{coil}} = \nabla \times \vec{A}_{\text{coil}} \quad (4)$$

The magnetic vector potential  $\vec{A}_{\text{coil}}$  can be written for a single current loop using the spherical coordinate system as [8]:

$$\vec{A}_{\text{coil}} = \frac{m_o m_o \sin q}{4a^2 p} \vec{a}_\phi \quad (5)$$

where  $m_o$  is the magnetic dipole moment,  $\vec{a}_\phi$  is the unit vector in spherical coordinates in the direction- $\varphi$  at an arbitrary position. Through these equations, the gradient of the magnetic flux density  $\partial \vec{B}_{\text{coil}} / \partial x$  can be obtained through partial differentiation of the equation.

Finally, the attractive magnetic force,  $\vec{F}_{\text{mag}}$  on a single particle in a non-uniform magnetic field is obtained by applying the following vector equation [6]:

$$\vec{F}_{\text{mag}} = \frac{1}{2} \chi_v V \vec{B}_{\text{ext}} \frac{\partial \vec{B}_{\text{coil}}}{\partial x} \quad (6)$$

where  $\vec{F}_{\text{mag}}$  is the magnetic force acting on a particle in the x-direction. When the microbead is suspended in a fluid environment, it experiences a hydrodynamic drag force. Assuming there is no fluid flow in the suspension, the hydrodynamic interaction can be modeled by Stoke's Law for the drag on a sphere. The force is a velocity-dependent viscous drag on the sphere of radius  $R_{\text{bead}}$ , given by [9]:

$$\vec{F}_{\text{drag}} = 6R_{\text{bead}} \pi \vec{h} v \quad (7)$$

$\vec{F}_{\text{drag}}$  is the drag force on a sphere,  $\eta$  is the viscosity of the fluid and  $\vec{v}$  is the terminal velocity of the bead within the fluid. Due to the spherical shape of the bead, chemical agglutination is minimized and the magnetic interactions between these beads are not considered. Furthermore, the effect of gravity is neglected due to the small mass of the particle [9]. The resulting equation of motion for a spherical particle balances the magnetic force and viscous drag term:

$$\vec{F}_{\text{mag}} = \vec{F}_{\text{drag}} \quad (8)$$

It is assumed that the gradient of the magnetic field is constant to yield the time-dependent equation for the position. Therefore the terminal velocity  $\vec{v}$  is given by:

$$\vec{v} = \frac{1}{12} \frac{\chi_v V \vec{B}_{\text{ext}}}{\pi R_{\text{bead}} \eta} \frac{\partial \vec{B}_{\text{coil}}}{\partial x} \quad (9)$$

The velocity of the bead can be maximized by reducing the drag force on the bead-cell composite, or by increasing the magnetic force on the beads. The trajectory,  $\vec{\Delta D}(t)$  of the bead traveling within a certain medium depending on the terminal velocity.

$$\vec{\Delta D}(t) = \vec{v} \Delta t \quad (10)$$

The viscosity of different fluids will be determined by measuring the time of flight,  $t_{\text{flight}}$  of the bead over the distance,  $D_{\text{inter}}$  ( $100\mu\text{m}$ ) between two microcoils. The equation is dependent on a constant magnetic force produced from a microcoil.

$$t_{\text{flight}} = \frac{6D_{\text{inter}} R_{\text{bead}} \eta \pi}{F_{\text{mag}}} \quad (11)$$

### 3 DESIGN

In order to optimize the device to produce large magnetic forces, it is necessary to maximize the gradient of the magnetic field while maintaining a constant external magnetic field,  $B_{\text{ext}}$ , large enough to ensure complete alignment and saturation of the magnetic beads. Therefore, the desirable parameters for an optimum design include the following factors:

- Generating high magnetic field gradients ( $10^3 \sim 10^4$  T/m)
- Permanent magnet with moderate magnetic field, (approximately 1 Tesla)
- Compatibility with optical microscope stage for easy visual monitoring
- Reasonable interelectrode spacing

The pattern of the microcoil shown in Figure 1(c) resembles a horse-shoe and it is fabricated on a silicon wafer with an area of  $5 \times 3 \text{ cm}^2$ . The coil has an outer radius,  $R_o$  of  $16 \mu\text{m}$  and an inner radius,  $R_i$  of  $8\mu\text{m}$ . The width of the track is  $8\mu\text{m}$  and it is  $1 \mu\text{m}$  thick. There are 3 coils arranged in series, separated at a distance of  $100\mu\text{m}$  from one another. Marks on the side of the chip spaced at  $10\mu\text{m}$  will provide a scale for the velocity measurement.

The characterization chamber is used to channel the flow of beads through the fluid under test. It consists of a straight channel via an inlet and outlet ports where its length is 3 cm with a rectangular cross-sectional area of  $100 \times 100 \mu\text{m}^2$ .

The microrheometer is manufactured from two wafers one glass the other silicon. The two main steps involve in the processing of the electromagnetic coils are the image reversal and lift-off process. The main purpose of using the image reversal process is to obtain negative slope profiles which provide a primary need for lift-off processing when tight linewidth control is required. Initially, a layer of positive tone film resist (AZ5214 E) is spun on the silicon wafer to a thickness of  $1\mu\text{m}$ .

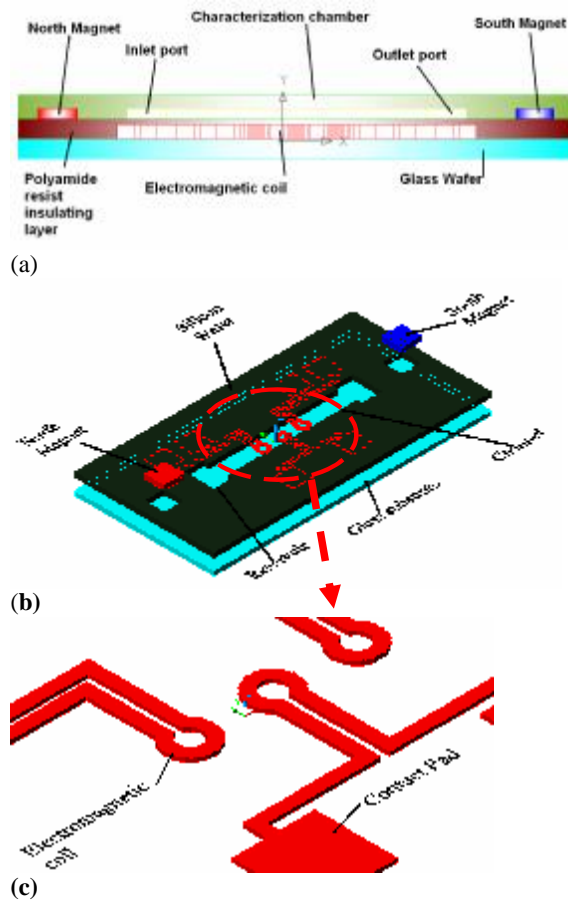


Figure 1: Schematic view of the microrheometer

The image reversal (IR) process converts the polarity of AZ5214E resist to negative resist, through multiple UV exposure of the wafer on a mask aligner. A number of baking stages is also required to alter the composition of the resist. During the developing stage, unwanted resist is dissolved using AZ726 MIF. A test pattern of the design is shown on Figure 2(a). A layer of chromium (Cr) is deposited to form a seed layer for the gold tracks (Au) during thermal evaporation process. When the coating process is completed, the wafer undergoes a lift-off process leaving behind the horseshoe coil (Figure 2(b)). A layer of polyamide resist is spun to a thickness of 2 $\mu\text{m}$  to provide an insulating layer for the coils.

The next step involves fabricating the characterization chamber for flow of the fluid on a silicon wafer. The characterization chamber consists of a microfluidic channel via inlet and outlet ports. The cavities for the permanent magnets are located on both ends of the chamber. Initially, a layer of AZ5214E resist is spun on the surface of the silicon wafer. The pattern of the characterization chamber is transferred on the resist layer using UV photolithography on a mask aligner. The pattern is etched on the silicon wafer using a deep reactive ion etch (DRIE) process on an STS 100 ICP etcher. When both wafers are manufactured, the glass and silicon wafers are

bonded together through anodic bonding.

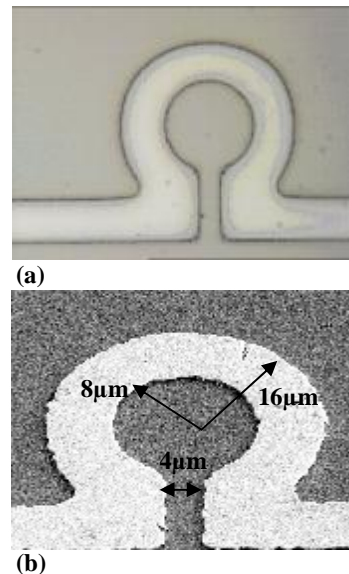


Figure 2: (a) Single loop coil fabricated using photolithography; the width of the track is 8 $\mu\text{m}$ . (b) SEM image of a single coil deposited with gold fabricated from lift-off process.

## 4 RESULTS

A theoretical model was set-up to evaluate the velocity of the bead for a given fluid viscosity. To obtain the velocity, the gradient of the magnetic flux density,  $\frac{dB_{\text{coil}}}{dx}$  is obtained from:

$$\frac{dB_{\text{coil}}}{dx} = \frac{3}{4} a^2 \mu_0 \left[ \frac{-5x^2 z}{(x^2 + z^2)^{7/2}} + \frac{z}{(x^2 + z^2)^{5/2}} \right] \quad (12)$$

where  $x$  is the distance from the center of the coil and  $z$  is the height at which the magnetic flux density is measured at an arbitrary position. For a single loop coil, the average coil radius is measured at  $a = 12\text{mm}$  and the current passing through the coil is  $I = 1\text{mA}$ . The result for the gradient of the magnetic flux density is shown in Figure 3. The average gradient of the magnetic flux density is:

$$\frac{dB_{\text{coil}}}{dx} = 3046 \text{ T/m} \quad (13)$$

From Equation 6 the magnetic force acting on a single bead at  $B_{\text{ext}} = 1 \text{ Tesla}$  is:

$$\overrightarrow{F_{\text{mag}}} = 1.735 \text{ f N} \quad (14)$$

The terminal velocity,  $v$  from Equation 9 taking the viscosity of water,  $\eta_{\text{water}} = 1.002 \times 10^{-3} \text{ kg/ms}$ .

$$v = 2.736 \text{ } \mu\text{m/s} \quad (15)$$

Equation 9-11 are repeated for a range of fluids to determine its effect of the viscosity on the terminal velocity of the bead and the distance traveled over  $t = 1$  second (see table 1). Using equation 11 we can measure the time of flight for various viscosities demonstrated in Figure 4. Equation 9 and equation 10 have also been used to give the various times the beads will take to travel a predetermined distance when contained in different fluids. Such data can be used to characterize and identify unknown fluids.

Fluid	Viscosity, $\eta \times 10^{-3}$ (kg/ms)	Velocity, $v \times 10^{-6}$ (m/s)	Distance at $t=1$ s, $D \times 10^{-3}$ (m)	Time flight at $D_{\text{inter}} = 100 \mu\text{m}$ , $t_{\text{flight}}$ (s)
Water	1.002	2.736	1.37	36.54
Milk	1.1526	2.738	1.19	42.04
Pentane	0.2143	1.279	6.402	7.8168
Butyric Acid	2.208	1.241	0.62	80.54

Table 1: Comparison of various fluid viscosities

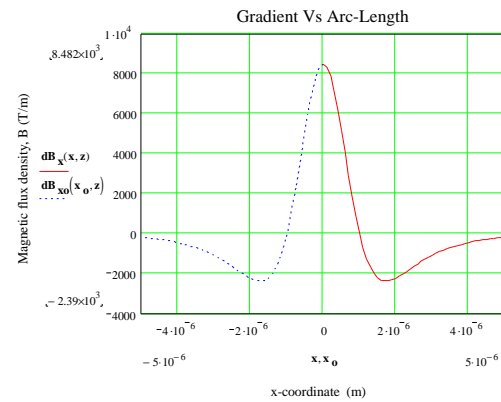


Figure 3: Magnetic flux density, versus x-coordinate for a single loop of coil.

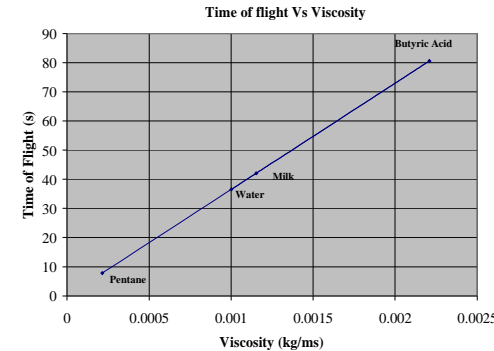


Figure 4: Time of flight for beads in different fluids within the device.

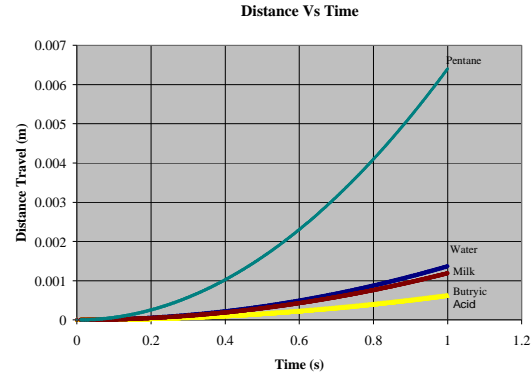


Figure 5: Distance traveled Vs Time at  $I = 1$  mA.

## 5 CONCLUSION

A microrheometer capable of measuring viscosity of measuring viscosity for microquantities of test fluid has been designed and modeled for a range of different fluids. The basic concept involves time of flight measurements for superparamagnetic microbeads driven by the fields from electromagnetic coils. A fabrication route involving optical lithography, metal deposition and deep reactive ion etching is proposed. Test "horseshoe" coils have been fabricated and will form the basic of a test cell to be made shortly. Further, modeling is planned using the FEMLAB FEA package.

## REFERENCES

- [1] V.Breedveld, D.J Pine J. Mat. Sci. **38**, 4461-4470, 2003.
- [2] F.Ziemann, J.Radler and E.Sackmann. Biophys. J. **66**(6), 2210, 1994.
- [3] Ashkin, Proc. Nat. Acad. Sci. USA. **94**(10), 4853, 1997.
- [4] B.Y. DU et al., Langmuir **17**(11), 3286, 2001.
- [5] R. E. MAHAFFY, et al., Phys. Rev. Lett. **85**(4), 2000.
- [6] B.I.BLeaney, B.Bleaney, "Electricity and Magnetism", Oxford Uni. Press, London, 1965.
- [7] L.Solymar, D.Walsh, "Lectures on the Electrical Properties of Materials," Oxford Sci. Pub., New York, 1970.
- [8] Clayton R. Paul and Syed A. Nasar, "Introduction to Electromagnetic Fields," McGraw Hill, New York, 1987.
- [9] Chong H. Ahn, Mark G. Allen, William Trimmer, Yong-Nam Jun and Shyamsunder Erramilli, J. of MEMS Syst., 5 No.3, 1996.